MAGNETIC FIELD CONFIGURATION ASSOCIATED WITH SOLAR GAMMA-RAY FLARES IN JUNE 1991

M. J. Hagyard,[1] E. A. West,[1] J. E. Smith,[1] F.-M. Trussart,[2] and E. G. Kenney,[3]

Abstract: In this paper we describe the vector magnetic field configuration of the solar active region AR 6659 that produced very high levels of flare activity in June 1991. The morphology and evolution of the photospheric fields are described for the period June 7 to June 10, and the flares taking place around these dates and their locations relative to the photospheric fields are indicated. By comparing the observed vector field with the potential field calculated from the observed line-of-sight flux, we identify the nonpotential characteristics of the fields along the magnetic neutral lines where the flares were observed. These results are compared with those from an earlier study of γ-ray flares.

1. Introduction

In early June of 1991, the Sun produced some of the most intense solar flares of the present cycle of activity. These events were particularly significant for several reasons. First, there were a number of very large flares, five of which produced x-ray fluxes that saturated the NOAA GOES detectors. Second, the Gamma Ray Observatory mission was in progress and the Principal Investigators made the decision to make the Sun a target of opportunity in anticipation of the high level of activity. And finally, a coordinated campaign of ground-based observations was organized to observe the activity in all possible wavelengths.

The Marshall Space Flight Center (MSFC) Solar Observatory took part in this campaign and observed the active region (NOAA AR 6659) responsible for the high level of activity from June 2 through June 10. The primary instrument of the observatory, the MSFC vector magnetograph (Hagyard et al., 1982, 1985), obtained measurements of the magnetic field of AR 6659 for 7 days, June 4-10. For several of these days, vector magnetograms were obtained over a 10-hour period so the temporal evolution of the magnetic fields was well documented.

While the correlation of this evolution with the flare activity was of interest, our main emphasis in the observational program was to document the nonpotential characteristics of the magnetic field and their relation to the occurrence of γ-ray flares. This latter theme is the

---

[1]Space Science Laboratory, NASA, Marshall Space Flight Center
[2]Ecole Normale Supérieure de Lyon
[3]Boeing Integrated Information Services

basis of the MSFC GRO Guest Investigation so the June active region served as an excellent subject for this study.

In this paper, we will describe our progress in this Guest Investigation, starting first with a description of the active region, the morphology and evolution of its magnetic fields, and the flares and their locations relative to the fields. We will then describe the nonpotential features of the field for the period June 7-10 and relate them to the flare locations. Finally, we will analyze these nonpotential characteristics in the context of previous studies of γ-ray flares.

2. Observations of the Active Region

The region was very large in area, visible to the naked eye, in fact. Mt. Wilson sunspot data (T. Shieber, private communication) indicated that two umbral areas in the active region had field strengths ≥ 3000 G. The region was located at a high solar latitude ($31°$ N), a location that has produced several difficulties in interpreting the observed vector magnetic field.

Numerous flares were observed to occur in this region during its disk passage; a total of 26 M-class and 6 X-class flares made up the list of "energetic" events. In Table 1 the relevant data on the X-class flares are listed (SESC/NOAA Preliminary Report and Forecast of Solar Geophysical Data 822-824).

Table 1. Major Flares in AR 6659, June 1991

Date	Time (UT)			X-Ray	Imp	Location	Radio
	Begin	Max	End				
June 1	1456	1520	1726	X12	1F	N25E90	II/IV
June 4	0337	0352	0800	X12	3B	N30E70	II/IV
June 6	0058	0108	0431	X12	4B	N33E44	II/IV
June 9	0134	0143	0152	X10	3B	N34E04	II/IV
June 11	0156	0209	0220	X12	3B	N31W17	II/IV
June 15	0810	0821	1402	X12	3B	N33W69	II/IV

Except for the June 1 event which could not be observed since it was literally at the east limb, all these flares occurred during the night at MSFC. As a consequence we did not obtain any magnetic field observations just before, during, or after these flares and we have had to rely on H-α data from other observatories to locate the flares within the region. The flare of June 9 is shown in Figure 1; these images were provided by the Big Bear Solar Observatory. This figure shows that the main emission in the flare was located in the northeastern part of the active region. Images of the flare on June 6 show this was also the area of the main emission in H-α for that flare. However, a 3B/M4 flare on June 7 was observed in the western part of the region.

0143 UT

0143 UT

Fig. 1. The 3B/X10 γ-ray flare of June 9, 1991. Images courtesy of Big Bear Solar Observatory.

An analysis of the morphology and evolution of the magnetic field from magnetograph observations showed that changes were taking place at these flare locations in the northeastern and western areas. The line-of-sight (LOS) component of the field over the period June 7-10 is shown in Figure 2. The area of maximum negative (black) polarity was the location of the largest umbrae in the region; these umbrae typically had maximum field strengths of 2800-3000 G. The area of maximum positive (white) polarity was associated with a single umbra in the northeastern part of the region; it had a maximum field strength of $\approx$3000 G. Very steep gradients were observed along the eastern "neutral line" separating positive and negative fields.
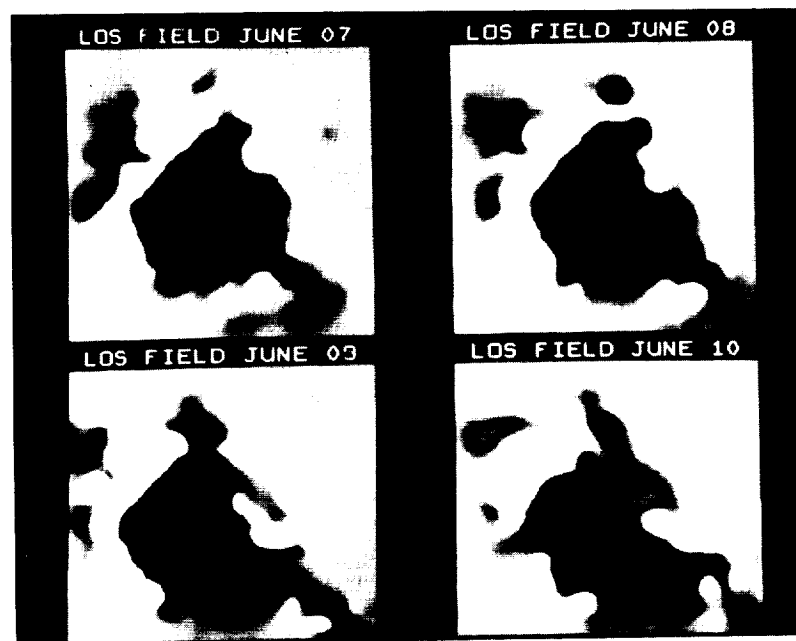

Fig. 2. Line-of-sight fields in AR 6659 for June 7-10. The grayscales run between ± 1500 G. North is up; west is to the right. The field of view is 2.8′ × 2.8′.

Several changes in the LOS field are seen over the time period June 7-10. The positive fields along the eastern neutral line are seen to change, notably from June 9 to June 10. Also, the area of negative polarity to the east of these positive fields that intrudes into the positive polarity is seen to disappear during this same interval. There is a notable development of the negative polarity in the northern part of the active region, particularly from June 7 to June 8. In the western part of the region one sees numerous changing patterns in both positive and negative polarities.

There is a caveat that must be kept in mind when looking at these changes: projection effects may be a source of some of them because of the high latitude of the region. However, these areas where the changes were occurring were also the locations of many of the flares

observed; this fact is a strong argument for believing that significant changes were taking place there.

The total vector field is represented in Figure 3 by superimposing the transverse field on the LOS fields of Figure 2. The strength of the transverse field is represented by the length of the line segments, and the direction (azimuth) of this field is indicated by the orientation of the segments.

The evolution of the transverse field is most notable in the same areas where the LOS field was changing. The positive fields in the southeastern area of the region weaken and change direction from June 9 to June 10, in step with the breaking up of the positive fields and the intrusion of negative polarity there. In the northern area where negative polarity develops from June 7 to June 8, the transverse field reconfigures with the azimuth of the field rotating almost 90°. In the western part of the region from June 9 to June 10 the field grows and rotates direction along the neutral line near the intrusion of positive polarity. Again, these changes are occurring in the areas where flares were observed.

3. Nonpotential Characteristics of the Magnetic Field

The strong magnetic field throughout a solar active region is believed to be the source of the energy released in a solar flare. If this is true, then the field must be in a configuration in which energy is stored in the field. If the field was a potential field, there would be no energy for release in a flare since the potential field represents the lowest energy state possible for a given distribution of flux over the surface. If the configuration of the potential field was known, then a comparison of it with the observed field would provide a measure of how "nonpotential" the real field is and thus an indication of stored energy.

This idea is the basis for our analyses of the nonpotential characteristics of the field of AR 6659. We use the distribution of the normal component of the field to calculate the potential field, using the method of Teuber et al. (1977) and compare its transverse component with that of the observed field. Such a comparison is shown in Figure 4 for the fields observed on June 9. The magnetic neutral lines are indicated by the dark lines; these mark the areas where flares generally occur. A comparison of the azimuths of the observed and potential fields show there are large discrepancies between them along the marked neutral lines. Indeed, the potential field is seen to cross the neutral line perpendicularly in these areas whereas the observed field lies almost parallel to the neutral lines. We refer to this difference between the potential and observed azimuths as angular "shear," $\Delta\phi$, and infer that the fields are highly stressed in these configurations. Thus, we believe this configuration of photospheric fields is an indication that magnetic energy is stored in these fields and can be released in the form of flares.

In previous studies of stressed fields in other active regions, we have developed quantitative measures of the angular shear (Hagyard et al., 1984; Hagyard and Rabin, 1986; Hagyard, 1990). Selecting those pixels that lie along the main magnetic neutral lines of an active region, we compute $\Delta\phi$ for those points that have field strengths B fitting the criteria 300 $G \leq B$ and $B^*/2 \leq B$, where B^* is the maximum field strength along the selected neutral line.
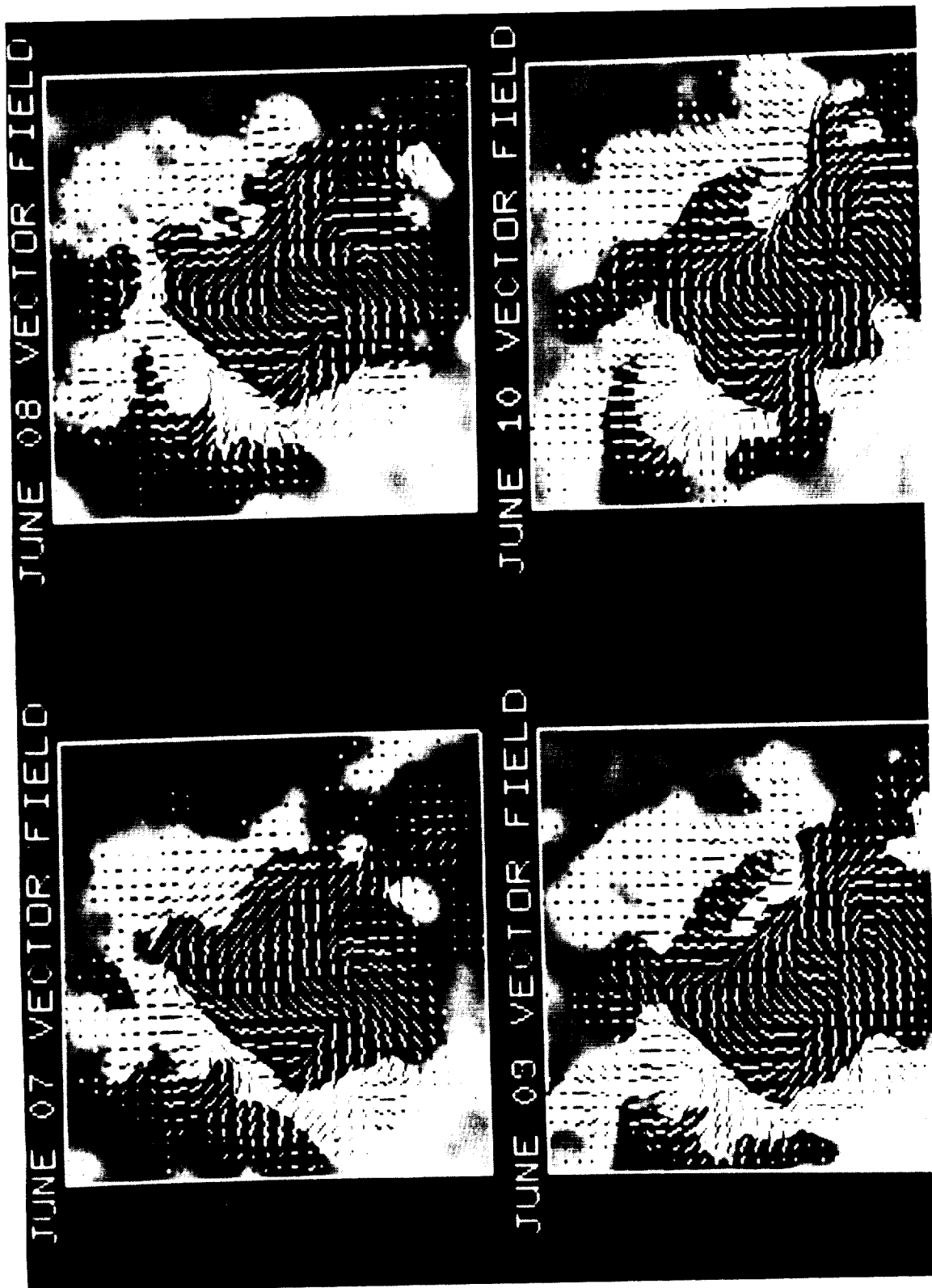
Fig. 3. Vector fields in AR 6659 for June 7-10. The grayscale represents the line-of-sight component of the field. The transverse component is represented by the line segments with scaling between 100 and 500 G.
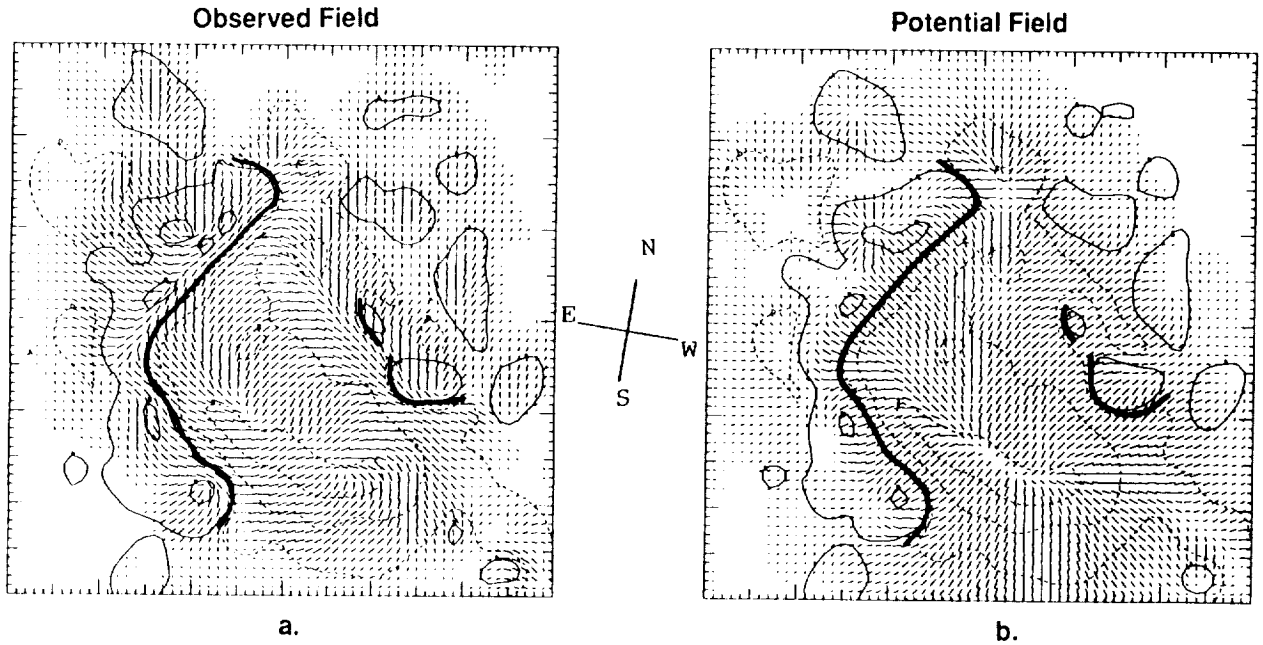
Observed Field   Potential Field

a.   b.

Fig. 4. The observed field and (computed) potential field in AR 6659 for June 9. Contours
represent the line-of-sight field; line segments represent the transverse field. The main
neutral lines are indicated by the dark contours.

Then we designate points to be moderately stressed if

$$70° \leq \Delta\phi < 80°$$

and highly stressed if

$$80° \leq \Delta\phi \leq 90°.$$

(In our definition of angular shear, 90° represents the maximum value attained by $\Delta\phi$.) Maps of
these points of stress are made by using symbols for the two different ranges of $\Delta\phi$: + and * for
the moderately and highly stressed points, respectively. Examples of "shear" maps for
observations taken June 7-10 are shown in Figure 5. The shear map for June 9 (Figure 5c)
illustrates quite graphically the differences seen in Figure 4 between the observed and potential
fields. In particular, notice the line of seven contiguous points of high angular shear along the
eastern neutral line and a longer one along the western neutral line for June 9. These extended
lengths of shear indicate large areas of stressed fields at these locations and are signatures we
have found in other active regions that produced big flares (Hagyard, 1990).

The analyses for nonpotential fields leading to the results shown in Figures 4 and 5 are
not precisely correct since we did not take projection effects into account. An exact calculation
of the potential field using the method of Teuber et al. (1977) requires the use of the true
normal-to-the-surface component of the field rather than the line-of-sight one. With this region
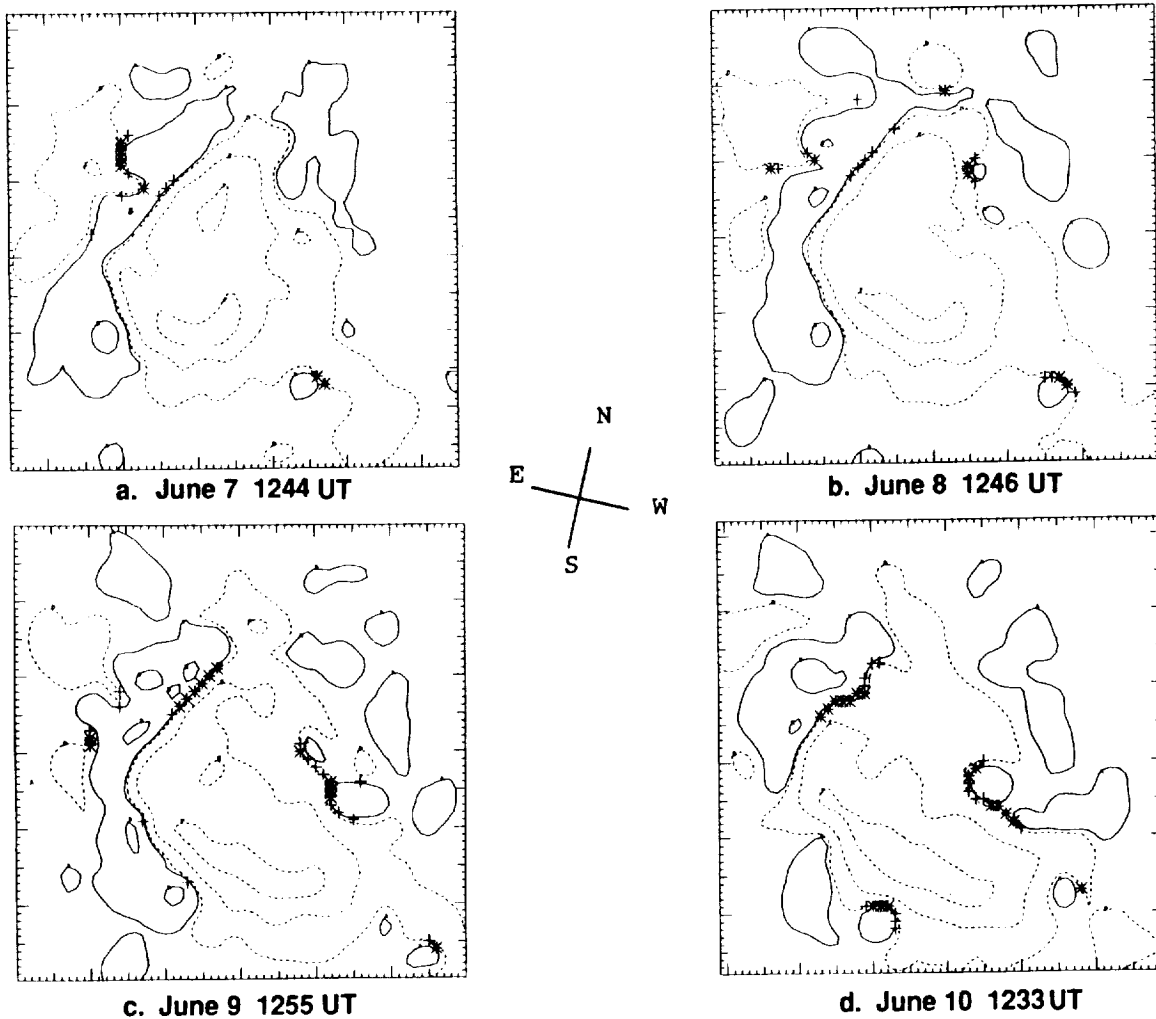
Fig. 5. Areas of strongly nonpotential fields along the neutral lines in AR 6659. Contours represent the line-of-sight component of the magnetic field. The symbols are defined in the text.

located at such a high latitude, the line-of-sight component is a poor approximation for the potential calculation. Projection effects will also change the neutral lines and thus the evaluation of shear along neutral lines (Gary and Hagyard, 1990).

To evaluate the nonpotential characteristics correctly, the measured field must be transformed into heliographic coordinates (Hagyard, 1987; Venkatakrishnan et al., 1988). However, to carry out this transformation, the ambiguity of 180° in the azimuth must be resolved. For complex active regions where the field is highly sheared, such as AR 6659, it is extremely difficult to determine the true direction of the transverse component. The methods we employ for this determination include comparisons with the direction of the potential field, comparisons with H-α structures, and connectivity between positive and negative fields *in heliographic coordinates*.

497

At this time we have performed this exercise to resolve the ambiguity in the azimuth for the observations of June 8 and 9 only. In Figure 6, the vector field for June 9 is shown in the image plane and heliographic coordinates. Note that the image plane field in this figure is identical with Figure 4a, except that now the line segments are given directions. Changes in the morphology of the magnetic field are evident as a result of the transformation. Such changes underscore the importance of the heliographic transformation in studying the evolution of the fields as a region transits the solar disk.

Heliographic shear maps for June 8 and 9 are shown in Figure 7. Several significant changes from the image-plane shear maps of Figure 5 are seen. For June 8, the major change is the increase in shear along the western neutral line; also, the magnitude of the angular shear has increased on the eastern neutral line at the same pixel locations. For June 9, the major change is the additional shear along the southern (lower) section of the eastern neutral line.

Looking at the magnitudes of field intensity (B) and angular shear ($\Delta\phi$) along the entire eastern neutral line, we find maximum field and shear of 1480 G and 89°, respectively, on June 8; for June 9, the maxima are found to be 1720 G and 87°. For the western neutral line, the maxima are 1765 G and 89° on June 8 and 1720 G and 89° on June 9. (The data for June 8 and 9 were calibrated for maximum fields of 2500 G. Subsequently, data from Mt. Wilson indicated maximum fields of $\approx$ 3000 G. Thus, the values given here are underestimates.)

The 3B/X10 flare shown in Figure 1 started about 13 hours after the observations that produced the shear map for June 8 and 11 hours before those for June 9. Within the accuracy of the observational data, there certainly does not seem to be any noticeable change in the degree of shear as a result of this flare. However, there can be no doubt that the magnetic field was highly sheared in the area where the flare erupted.

4. Discussion

In an earlier study, we analyzed the nonpotential characteristics for a small sample of flare-productive active regions observed by the Gamma Ray Spectrometer on the Solar Maximum Mission (Hagyard et al., 1990). Using the same quantitative analysis for angular shear, we compiled the data given in Table 2.

Table 2. Comparison of Nonpotential Parameters

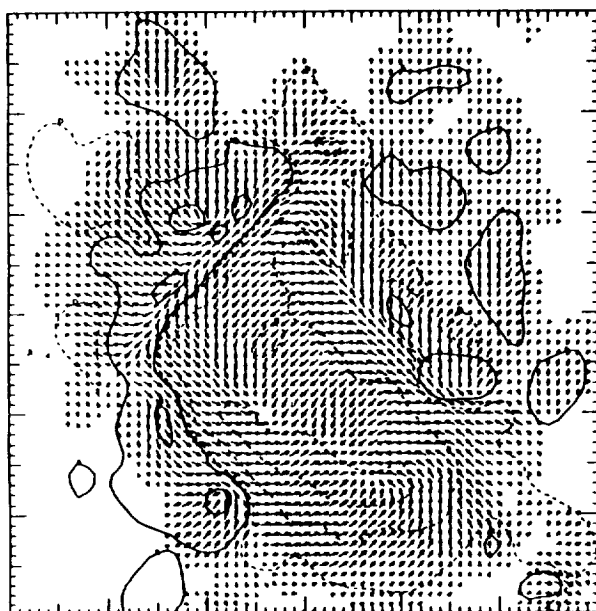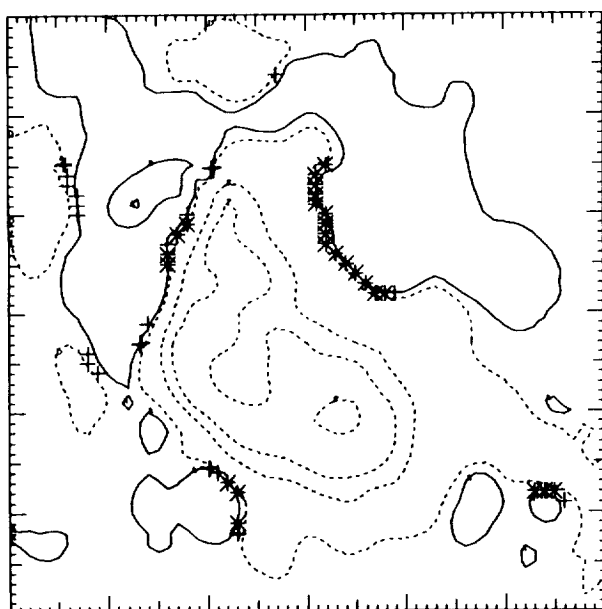| Date of Flare	Max B (G)	Max $\Delta\phi$(°)	No. Points	Flare Class	γ Event
04/24/84	1700	90	15	3B/X13	yes
04/28/84	1920	90	8	2B/C6	no
02/04/86	1100	90	10	3B/X3	yes
11/05/80	1000	88	8	1B/M2	no
04/07/80	1000	85	8	1B/M4	no

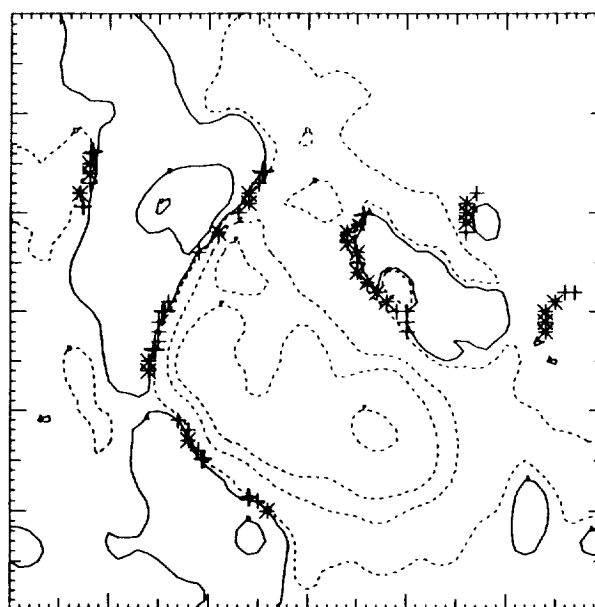IMAGE PLANE   HELIOGRAPHIC PLANE

Fig. 6. June 9 vector field in image plane and heliographic coordinates.

JUNE 8   JUNE 9

Fig. 7. Heliographic shear maps for June 8 and 9.

In this table, the numbers in the column "No. Points" indicate how many ≈ consecutive pixels along the neutral line are found in the area of maximum angular shear that satisfy $70° \leq \Delta\phi \leq 90°$ (i.e., ≈ consecutive pixels represented by + or *).

A similar table can be compiled for the data analyzed so far for AR 6659, although information about the flares occurring around the dates June 8 and 9 is limited to the one event along the eastern neutral line at 0134 UT on June 9. In this table, nonpotential parameters are given for the two separate neutral lines (NL in the table).

Table 3. Nonpotential Parameters for AR 6659

Date	NL	Max B (G)	Max $\Delta\phi(°)$	No. Points	Flare Class	γ Event
06/08/91	Northeast	1480	89	6	3B/X10	yes
	West	1765	89	16	??	??
06/09/91	Northeast	1720	87	7	3B/X10	yes
	Southeast	1335	84	8	same	yes
	West	1720	89	14	??	??

In the earlier study, the conclusion was made that the strength of the field along the neutral line and the corresponding degree of shear do not differ significantly between flares that produce γ-ray events and those that do not. However, it was also concluded that perhaps the extent of the nonpotential fields was a distinguishing factor, i.e., the number of consecutive pixels, since the two γ-ray events had somewhat larger numbers of consecutive pixels. Looking at the preliminary data in Table 3 for AR 6659, we see the same high field strengths and large angular shears that appear in Table 2. However, the number of consecutive points along the eastern neutral line is smaller than the numbers cited for the γ-ray flares in the earlier study. At first glance, the conclusion of that study needs to be re-examined based on the June 8 and 9 data. Perhaps when all the available magnetic observations for this active region have been analyzed, a clearer picture will emerge. Indeed, the goal of the MSFC Guest Investigation is to analyze observations for all active regions producing M-class or greater flares since the launch of GRO, classify these flares according to their productivity of γ-rays, and look for distinguishing characteristics in the nonpotential fields that correlate with these flares. At the end of this study, perhaps a more definitive set of criteria will emerge. Certainly, in June 1991, Mother Nature provided us with an excellent opportunity to begin this investigation.

5. References

Gary, G. Allen, and Hagyard, M. J.: 1990, *Solar Phys.* **126**, 21.
Hagyard, M. J.: 1987, *Solar Phys.* **107**, 239.
Hagyard, M. J.: 1990, *Mem. S. A. It.* **61**(2), 337.

Hagyard, M. J., and Rabin, D. M.: 1986, *Adv. Space Res.* **6**(6), 7.

Hagyard, M. J., Cumings, N. P., and West, E. A.: 1985, in *Proceedings of Kunming Workshop on Solar Physics and Interplanetary Travelling Phenomena*, C. De Jager and Chen Biao (eds.), Science Press, Beijing, China, p. 204.

Hagyard, M. J., Venkatakrishnan, P., and Smith, J. B., Jr.: 1990, *Astrophys. J. Suppl.* **73**, 159.

Hagyard, M. J., Cumings, N. P., West, E. A., and Smith, J. E.: 1982, *Solar Phys.* **80**, 33.

Hagyard, M. J., Smith, J. B., Jr., Teuber, D., and West, E. A.: 1984, *Solar Phys.* **91**, 115.

Teuber, D., Tandberg-Hanssen, E., and Hagyard, M. J.: 1977, *Solar Phys.* **53**, 97.

Venkatakrishnan, P., Hagyard, M. J., and Hathaway, D. H.: 1988, *Solar Phys.* **115**, 125.